Received: 01 December 2023 | Revised: 15 December2023 | Accepted: 30 December2023
DOI: 10.48309/JMPCR.2024.428856.1052
Journal of Medicinal and Pharmaceutical Chemistry Research
SAMI

FULL PAPER

Novel electrochemical sensor of Cu(II) prepared by carbon paste-magnetic ion imprinted materials on screen printed carbon electrode

Ani Mulyasuryani[a] | Matlal Fajri Alif[b] | Rahadian Zainul[c,*]

[a]*Analytical Chemistry Laboratory, Department of Chemistry, Faculty of Mathematics and Natural Sciences, Universitas Brawijaya, East Java, Indonesia*
[b]*Department of Chemistry, Faculty of Mathematics and Natural Sciences, Andalas University, Padang, West Sumatra, Indonesia*
[c]*Department of Chemistry, Faculty of Mathematics and Natural Sciences, Universitas Negeri Padang, Padang, West Sumatra, Indonesia, Center for Advanced Material Processing, Artificial Intelligence and Biophysics Informatics (CAMPBIOTICS), Universitas Negeri Padang, Indonesia*

Magnetic Ion Imprinted Materials (MIIMs) have specific recognition capabilities so that they have been widely used for the manufacture of electrochemical sensors with high selectivity. In this study, an electrochemical sensor has been developed for the detection of Cu(II) by modifying the screen printed carbon electrode (SPCE) by carbon paste-copper(II)MIIM. MIIM is made of a mixture of Fe_3O_4@SiO_2 and Cu(II) 3-aminopropyl triethoxysilane complex. MIIM characterization was based on surface morphology, FTIR spectrum and electrochemical properties of the modified SPCE. At the pH 3, the cathodic peak current from the sensor increases linearly with the Cu(II) concentration in the range from 0 ~200 nM with a detection limit (S/N = 3) of 3 nM. In addition, the developed sensor exhibits high sensitivity is 0.49 μA/nM with an accuracy of (102.7 ± 1.5) %. The Cu(II) sensor can be applied to surface water samples.

***Corresponding Author:**
Rahadian Zainul
Email: rahadianzmsiphd@fmipa.unp.ac.id
Tel: + 62 812-6138-5385

KEYWORDS

Copper(II); 3-aminopropyl triethoxysilane; magnetic nanoparticles; ion imprinted materials

Introduction

The field of electrochemical sensors in contemporary sensing systems has experienced numerous advancements stemming from the progress made in microelectronics and microengineering. These developments have primarily led to the creation of smaller sensors with heightened sensitivity and selectivity, while also reducing production and maintenance expenses. The ongoing research on electrochemical sensors focuses on investigating novel materials to enhance their selectivity capabilities as well as improve detection limits. The study of material behavior at the nanometric scale has contributed significantly to advancements in research and the practical use of electrochemical sensors and electroanalytical methods. The exploration of material behavior at the nanometric scale, which deals with dimensions and tolerances of less than 100 nanometers, has been pivotal in driving forward research and practical applications in the realm of electrochemical sensors and electroanalytical methods. At this minute scale, materials often exhibit unique physical and chemical properties that differ significantly from their bulk counterparts. These properties include increased reactivity, strength, electrical conductivity, and specific surface area. In the context of electrochemical sensors, such nanoscale materials provide enhanced sensitivity and selectivity for detecting various analytes. The increased surface area at the nanoscale allows for a higher density of reactive sites, thereby improving the sensor's responsiveness to target molecules. In addition, the nanoscale manipulation of materials has led to the development of more compact, efficient, and versatile sensors, which are crucial for real-time monitoring and analysis in environmental, medical, and industrial applications. These advancements in nanomaterials have also enabled the miniaturization of electroanalytical devices, making them more portable and user-friendly, thereby expanding their use beyond traditional laboratory settings into field applications and personal healthcare devices. This intersection of nanotechnology and electrochemical sensing is a testament to how studying materials at the nanometric scale can fundamentally transform and enhance technological capabilities.

Electrochemical sensors, which are a type of chemical sensor, have emerged as leaders in this field and have successfully transitioned into commercial applications. These sensors have proven to be invaluable tools in various areas such as clinical analysis, industrial processes, environmental monitoring, and agricultural studies [1,2,3,4,5,6,7].

The sensor is comprised of two primary components: a recognition element which facilitates selective and specific binding with the target analyte, and a transducer responsible for transmitting information regarding the binding. Parameters such as response time, signal-to-noise ratio (S/N), selectivity, linear range, and limit of detection (LoD) are all key factors in determining the effectiveness of these sensor components in recognizing and detecting analytes accurately. Enhancing the conductive properties of the sensor surface is a fundamental approach employed in the construction of electrochemical sensors to facilitate efficient electron transfer between the analyte surface and working electrode. Extensive research has been conducted on modifying the composition of the working electrode as a means to enhance both selectivity and sensitivity in electrochemical analysis. The working electrode plays a crucial role in amperometric and voltametric electrochemical sensors. Carbon-based electrodes, including carbon paste electrodes, glassy carbon electrodes, pencil graphite electrodes, screen printed electrodes, as well as metal-based gold electrodes, are commonly utilized and modified for this purpose [8,9,10,11,12,13].

Electrode surface modification can take the form of various techniques, including the application of an electroactive thin film, a single layer deposition method or a thicker layer created through strategies such as drop-casting [10,14,15,16,17]. Utilizing modified electrodes

in voltametric analysis offers several advantages, including exceptionally low detection limits, enhanced selectivity and the capability to simultaneously determine multiple analytes [18,19,20,21]. Extensive research has been conducted on the advancement of electrochemical sensors for Cu(II) detection. This includes both conventional methods as well as contemporary approaches with and without modification [22,23,24,25,26,27].

Copper holds significant importance in various metabolic processes, making it an essential element for most organisms. Nevertheless, when present in high concentrations, copper can have detrimental effects on living organisms. Prolonged exposure to the elevated levels of copper in humans may lead to various adverse health issues including stomach discomfort, dizziness, vomiting, and diarrhea. In addition, excessive absorption of copper can result in liver and kidney damage as well as potentially fatal outcomes. As a result, there is a need for analytical methods with high sensitivity and low detection limits when determining the concentration of Cu(II) [28,29,30,31]. Two techniques commonly used for this purpose are coupled plasma emission spectrometry [32], and atomic emission spectroscopy [33]. However, these methods pose challenges due to their reliance on large instruments, costly maintenance requirements, and skilled operators.

In recent times, there has been a significant surge in research focused on ion-imprinted polymers for the detection of Cu ions [34,35]. This approach offers a straightforward design, excellent sensitivity, and a remarkable low detection limit [1,27] when it comes to determine Cu. Furthermore, the utilization of Cu(II) imprinted polymers [36,37,38] in fabricating ion-selective electrodes highlights their distinctive features and wide range of applications in this field [25,26].

Ion-imprinted technology (IIT) emerged as a natural progression of molecular imprinting, sharing similar principles while focusing on ions as the templates. The synthesis of ion-imprinted polymers (IIP) typically involves various components such as template ions, functional monomers, crosslinkers, initiators, and solvents. In this context, the desired targets are usually specific ions that serve as templates for polymer formation. In the development and implementation process of IIP, various procedures are employed to combine template ions and functional monomers either through covalent or non-covalent bonding to create a pre-polymerization unit. Subsequently, polymers with significant cross-linking and rigidity are produced by utilizing initiators, cross-linking agents, as well as photoinitiated or thermally initiated polymerization techniques. In the end, the template ion is removed physically or chemically, resulting in a printed cavity that closely resembles both the size and structure of the template ion. These distinctive cavities exhibit high selectivity towards target ions through specific recognition mechanisms. To ensure the desired outcome of an IIP, careful consideration should be given to selecting the appropriate ion template, functional monomer, crosslinker, initiator, and solvent based on the target material [39,40,41].

While IIPs are known for their high selectivity, it is important to note that the incorporation of functional monomers and template ions within the polymer network can limit site accessibility for the target ion. Consequently, this may result in a reduced rate of mass transfer. To address this limitation, researchers have devised a method called surface ion-imprinted technology. This innovative approach utilizes supporting materials such as mesopore silica [42], MWCNT [43], and Fe_3O_4 [44] coated with a specialized polymer layer. This polymer layer possesses selectivity and effectively binds to the targeted metal ion through imprinting techniques.

The surface ion-imprinted polymer (SIIP) developed by SIIT has several advantages, including its high selectivity, increased

accessibility to binding sites, elevated adsorption capacity, and rapid mass transfer rate [45]. By creating the recognition site on the support's surface instead of deep embedding it, SIIP exhibits improved accessibility to target ions while avoiding complications associated with deeper embedding techniques [46]. Generally, SIIT have been extensively employed for the separation of metal ions in various studies [47,48]. In our research endeavor, we have utilized SIIT to create a Cu (II) ion sensor through the implementation of voltammetry. This study aimed to develop an electrochemical sensor utilizing SIIT. The inclusion of Fe_3O_4 as a core material facilitates the separation process during synthesis [49,50,51].

The presence of hydroxyl groups on the surface of Fe_3O_4 poses challenges in grafting onto it. To overcome this issue, a silica coating is applied to enhance both the grafting ratio and anti-acid capacity of this composite material. The production of magnetic ion imprinted polymer (MIIP) involves the silica polymerization on Fe_3O_4 surfaces, leading to a stable product that retains its structural integrity even in acidic conditions [52.53].

This study involved the modification of a silica layer onto the surface of iron oxide (Fe_3O_4@SiO_2) using the sol-gel method. This process began with the preparation of a sol, a colloidal mixture of precursors such as tetraethyl orthosilicate (TEOS) with water, alcohol, and a catalyst like hydrochloric acid or ammonia. The sol underwent hydrolysis and polymerization reactions, leading to the formation of a gel-like network that coated the Fe3O4 particles. As the gel solidified, it created a porous, silica-rich layer on the Fe_3O_4 surface, enhancing its chemical and physical properties. Subsequently, the Cu(II)-APTES complex was grafted onto this modified surface of Fe_3O_4@SiO_2 particles, also known as magnetic ion-imprinted material (MIIM). This method leveraged the unique advantages of the sol-gel process, such as controlled porosity and surface area, to improve the material's functionality in sensor applications. In recent studies, researchers have examined the application of Fe_3O_4 as a modifier in the working electrode to improve electrochemical sensors for detecting monosodium glutamate [54]. Furthermore, the inclusion of Fe_3O_4 in the nata de coco membrane has been found to enhance the potentiometric sensitivity of phenol sensors (Figure 1) [55,56,57].

The MIIM utilization as a modifier on the surface of screen-printed carbon electrodes (SPCE) offers a novel approach to enhance the sensitivity of electrochemical Cu sensors via voltammetry. This technique involves modifying SPCE with a molecularly imprinted polymer specifically designed for uric acid [58] and 4-aminophenol sensors, thereby improving their performance [59].

Methods

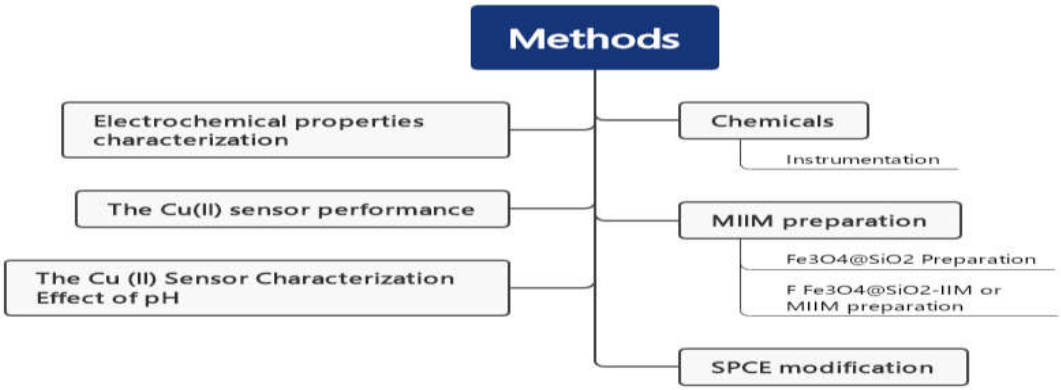

FIGURE 1 Flow diagram of this study

Chemicals

All reagents and chemicals utilized in this experiment were of analytical grade and were employed without any further purification. Carbon paste, Fe_3O_4, tetra ethyl ortho silicate (TEOS), 2-propanol, ammonia, copper sulfate, copper chloride, 3-aminopropyl tri ethoxy silane (APTES), methanol, and KCl were procured from Sigma-Aldrich in the United States. Sulfuric acid (H_2SO_4), hydrochloric acid, $K_3Fe(CN)_6$, $K_4Fe(CN)_6$, NaOH, KH_2PO_4, K_2HPO_4 from Merck; standard buffer at pH levels 4 and 7; as well as demineralized water was obtained for use.

Instrumentation

The Potentiostat/Galvanostat Autolab PGSTAT204 and DropSens µStat200 were utilized for the testing. Additional experimentation was conducted using a customized SPCE. The surface morphology of Fe_3O_4@SiO_2-IIM was assessed through SEM and FTIR analysis to evaluate the efficacy of synthesizing Fe_3O_4@SiO_2-IIM.

MIIM preparation

MIIM preparation refers to a procedure that has been developed by Luo *et al.* [22].

1. Fe_3O_4@SiO_2 Preparation

5 g Fe_3O_4 was added to 250 mL of 2-propanol and 2 mL of distilled water, sonicated for 15 min, and then added 20 mL ammonia and 33.3 mL TEOS, stirred for 12 h. Then, it is separated by a magnet. Then wash with distilled water until ammonia-free.

2. F Fe_3O_4@SiO_2-IIM or MIIM preparation.

a. 0.75 g $CuCl_2$ added 60 mL of methanol in a water bath and 4 mL of 3-aminopropyl tri ethoxy silane (APTES) stirred for 1 hour.

b. Fe_3O_4@SiO_2 of no. (1) is suspended into 50 mL of methanol, and then stirred and added to the mixture (a) above.

c. The mixture (a) and (b) is stirred for 24 hours at 40-50 °C.

d. Fe_3O_4@SiO_2 -IIM is separated with a magnet and washed with methanol and followed by HCl. 2 M and distilled water until HCl-free; check with litmus. Any Fe_3O_4@SiO_2 -IIM separation at the time of washing is magnetized.

SPCE modification

Three different combinations of mixtures can be used for modifying SPCE. These include a mixture containing equal amounts of carbon and MIIM in a 1:1 ratio, as well as a combination of 0.1 g each of MIIM and carbon, which is mixed with a few drops of paraffin oil and stirred to obtain a paste-like consistency. The paste was applied onto the surface of the working electrode on the SPCE, and subsequently dried at 50 °C for 10 minutes.

Electrochemical properties characterization

The electrochemical performance was evaluated through cyclic voltammetry on various sensor types including SPCE, SPCE-carbon paste, SPCE-MIIM, and SPCE-carbon paste-MIIM. To carry out the experiment, a 0.5 mM solution of $[Fe(CN)_6]^{3-/4-}$ in KCl (0.01 M) was utilized as a standard solution. The potential was set at -1.0-1.0 Volt and the scan rate ranged from 50 to 200 mV with increments of 25 mV (i.e., 50,75,100,125,150). CV measurements were conducted on a 100 µM Cu solution in 0.01 M KCl, with a potential ranging from -0.5 to 0.5 Volt. The diffusion coefficient was determined by conducting measurements at scan rates of 50, 75, 100, 125,150, and 200 mV.

The Cu (II) sensor characterization

Effect of pH

The influence of the pH of the supporting electrolyte on the voltammetric response of SPCE, specifically SPCE-MIIM and SPCE-C-MIIM, was investigated in a pH range from 2.0 to 5.0 with a Cu concentration of 100 µM. The pH adjustment was achieved using Briton Robinson

buffer solution. The measurements were conducted using CV (cyclic voltammetry) and SWV (square wave voltammetry).

The Cu(II) sensor performance

The evaluation of the proposed technique will involve an analysis of its linearity range and detection limit. The linearity range will be determined by observing the relationship between peak current and Cu(II) concentration, while the detection limit refers to the minimum value at which this relationship can be reliably detected. The concentration of Cu solutions was varied between 0.5-200 nM by dilution in a buffer solution at pH 3. SWV measurement with a frequency of 10 Hz and scan rate of 50 mV was conducted at a potential range of -0.5 to 0.2 Volt.

Results and Discussion

Characterization of magnetic ion imprinted material (Fe_3O_4@SiO_2-IIM)

The characterization of the magnetic ion imprinted material (Fe_3O_4@SiO_2-IIM) is demonstrated in Figure 2, where its FTIR spectrum is compared to that of commercial Fe_3O_4 utilized in this study. A noticeable distinction between the two spectra can be observed from the image. The FTIR analysis of Fe_3O_4 reveals a single peak at a wave number of 533 cm^{-1}, suggesting the existence of Fe-O bonds [60,61].

On the other hand, in the FTIR spectrum of Fe_3O_4@SiO_2-IIM, distinct peaks can be observed: one at 1620 cm^{-1} indicating the presence of a secondary amine group and others at 1043 cm^{-1}, 937 cm^{-1} indicating siloxane groups such as Si-O-Si or Si-O-C and silica ions, respectively [62,63].

The findings align with the SEM's EDX spectrum, suggesting that Fe, Si, O, and Cl are present in Fe_3O_4@SiO_2-IIM. The findings of the study, particularly in relation to the composition of the Fe3O4@SiO2-IIM (Iron Oxide at Silica-Ion Imprinted Material), show a strong correlation with the data obtained from the SEM's (Scanning Electron Microscopy) EDX (Energy-Dispersive X-ray) spectrum. The EDX spectrum, a technique used for elemental analysis or chemical characterization of a sample, revealed the presence of key elements: Iron (Fe), Silicon (Si), Oxygen (O), and Chlorine (Cl) in the synthesized material. Iron, being a primary component of Fe_3O_4, indicates the successful incorporation of iron oxide nanoparticles within the material's structure. Silicon and oxygen are indicative of the silica matrix, which is crucial for the stability and functionality of the ion-imprinted material. The presence of chlorine suggests the successful integration of chlorinated compounds or functional groups during the synthesis process, possibly from the precursors or catalysts used. This elemental composition confirms the successful formation of the Fe3O4@SiO2-IIM, with each element playing a critical role in the material's properties and its subsequent application in electrochemical sensing. The alignment of these findings with the SEM's EDX spectrum not only validates the material's composition, but also underscores the effectiveness of using advanced microscopic and spectroscopic techniques for material characterization in nanotechnology and sensor development.

In addition, Figure 3b indicates the release of Cu(II).

Electrochemical characterization

The $Fe(CN)_6^{3-/4-}$ 0.5 mM solution in 0.01 M KCl was subjected to CV measurements at different scan rates. The electrochemical reduction of ferricyanide ions to ferrocyanide and the subsequent oxidation process were performed on a SPCE electrode with a diameter of 3 mm, utilizing CV techniques at scan rates ranging from 50 mV s^{-1} to 200 mV s^{-1}. Figure 4 displays the typical cyclic voltammetry response for redox couples, specifically for a solution containing 0.5 mM potassium ferricyanide

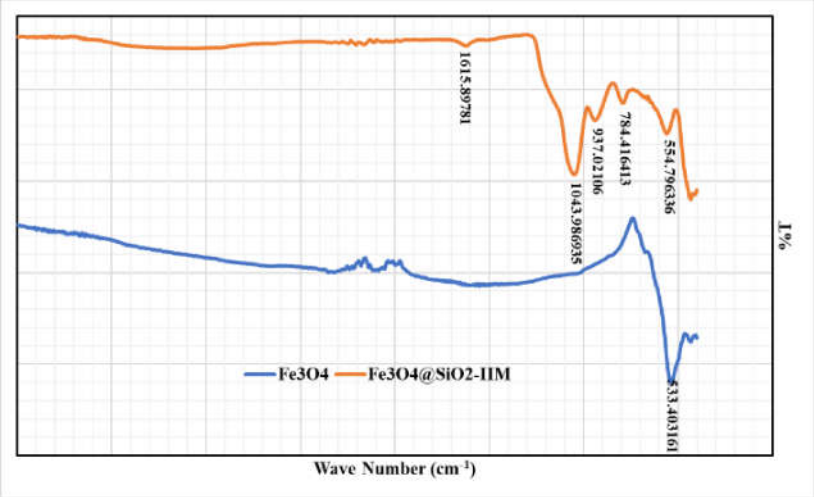

FIGURE 2 FTIR spectrum of Fe_3O_4 and Fe_3O_4@SiO_2-IIM

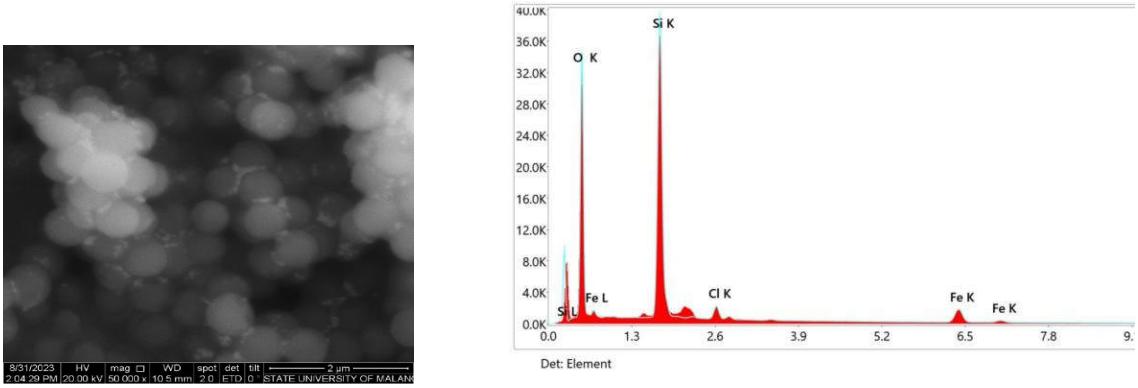

(a) (b)

FIGURE 3 Scanning electron microscopic image of MIIM (a) and EDX (b)

in a 0.01 M KCl solution. CV comprises of both an anodic sweep (forward sweep) and a cathodic sweep (reverse sweep). During the initial phase of the forward sweep, specifically before reaching 0.0 V, there is no occurrence of electrolysis.

However, once the voltage surpasses this threshold (0.0 V), an oxidation process initiates and gradually intensifies until it reaches its maximum value on the current-voltage curve. At this point, the graph showcases a distinct peak shape which suggests that the oxidation process becomes diffusion-limited. Following the continuation of the oxidation process, there is a decline in its rate. The overall outcome of this process involves the conversion of ferrocyanide into ferricyanide. The point at which the oxidation current reaches its highest magnitude is referred to as the anodic peak current (I_{pa}), while the maximum potential at that point is known as the anodic peak potential (E_{pa}).

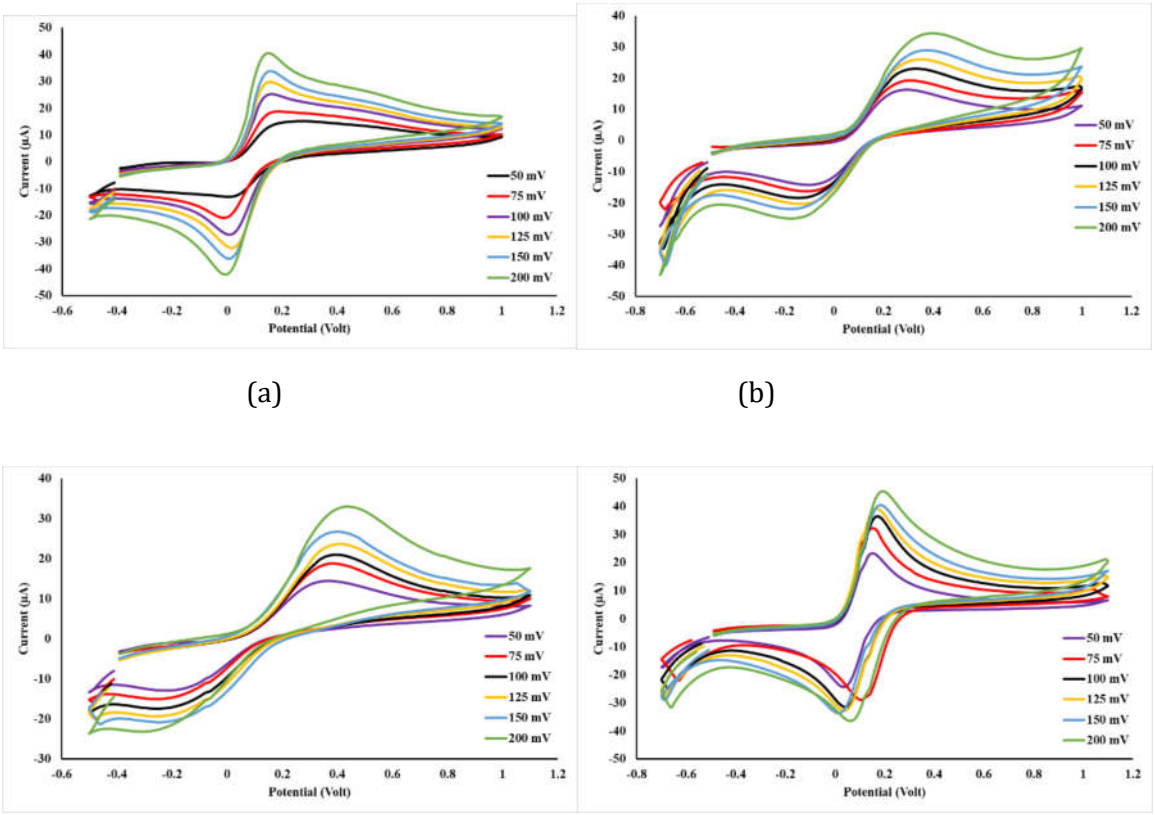

FIGURE 4 Cyclic voltammogram for $Fe(CN)_6^{3-/4-}$ 0,5 mM in 0,01 M KCl. SPCE (a); SPCE-C-MIIM (b); SPCE-MIIM (c); and SPCE-C (d)

The CV measurements yielded an E_{pa} value of 0.349 V and an I_{pa} value of 1.82×10^{-5} A. Interestingly, even in the reverse or cathodic sweep, the oxidation process still takes place followed by a subsequent reduction of $[Fe(CN)_6]^{3-}$ that reaches its maximum point where the CV once again exhibits a peak shape. During the reduction process, the system eventually reaches its diffusion limit. At this point, the value of E_{pc} is measured to be 0.195 V and I_{pc} is found to be 3.22×10^{-5} A. The reduction reaction then proceeds further. Analysis from a cyclic voltammetry experiment confirms that the redox reaction between ferricyanide and ferrocyanide involves the transfer of a single electron. The experiment involved conducting measurements on various electrodes, specifically SPCE; SPCE-C-MIIM; SPCE-MIIM; and SPCE-C. Based on the data presented in Figure 5, a curve was formulated to establish a relationship between the square root of the scan rate (ν) or $\nu^{1/2}$ and the cathodic and anodic peak currents for predicting the diffusion coefficient of $Fe(CN)_6^{3-/4-}$ for each sensor, as shown in Figure 5. According to Figure 4, analyzing the CV data and peak current values reveals that an increase in the scan rate leads to higher I_{pa} and I_{pc} peaks. This finding demonstrates a clear correlation between the peak current and scan rate, thereby confirming the relationship described in the Randles-Sevcik equation at 298.15 K.Where, n is the number of electrons involved in the redox half-reaction being studied, D is the diffusion coefficient for the redox active species, C is the molar concentration of the redox active species, A is the surface area of the electrode, and υ is the rate at which the potential is being swept [63,64,65,66].

$$I_p = (2.69x10^5)ACn^{3/2}D^{1/2}\vartheta^{1/2}$$

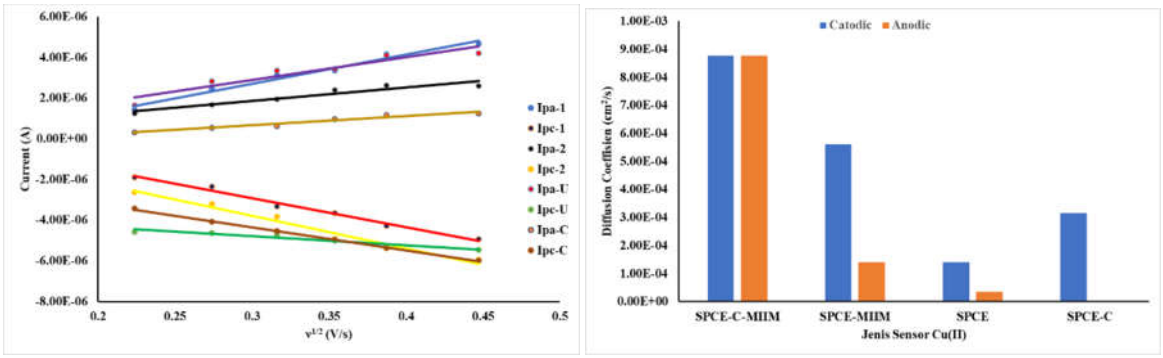

(a) (b)

FIGURE 5 Relationship curve between (scan rate)$^{1/2}$ and cathodic and anodic peak currents (a), cathodic and anodic diffusion coefficients of $Fe(CN)_6^{3-/4-}$ solution on the SPCE surface; SPCE-C-MIIM; SPCE-MIIM; and SPCE-C (b)

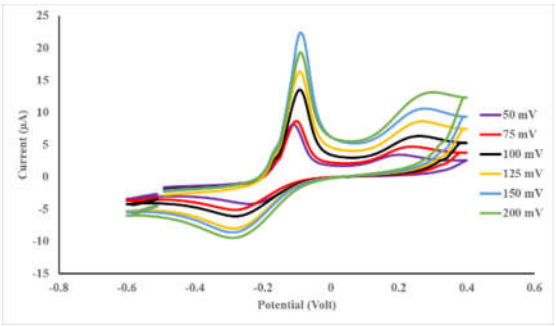

FIGURE 6 Cyclic voltammogram for 100µM Cu(II) solution in 0.01 M KCl solution, on SPCE-C-MIIM

According to the findings presented in Figure 5, it is evident that the diffusion coefficient for $Fe(CN)_6^{3-/4-}$ is highest when SPCE is modified with a combination of carbon paste-MIIM (SPCE-C-MIIM). As a result, this particular sensor exhibits the highest level of sensitivity. In consideration of the observed electrochemical properties of each sensor, it has been determined that the SPCE-C-MIIM sensor exhibits the highest sensitivity. Consequently, CV analysis was conducted on this particular sensor using a 100µM Cu(II) in a 0.01 M KCl solution.

Electrochemical analysis was also conducted on SPCE for the purpose of comparison, as demonstrated in Figure 6. The cyclic voltammogram of the Cu(II) solution in KCl revealed two distinct anodic peaks occurring at -0.14 and +0.2 Volts, indicating the presence of two oxidation states of Cu(II), that Cu(I) and Cu.

$$Cu^{2+} + e^- \rightarrow Cu^+ \qquad E^o = +0.153\, Volt$$

$$Cu^+ + e^- \rightarrow Cu \qquad E^o = +0.521\, Volt$$

When utilizing Ag/AgCl as a reference electrode in 0.01 M KCl solution (E = 0.346 Volts), the reduction potentials mentioned above are altered to -0.193 and +0.175 Volts, correspondingly. The current height observed at the initial reduction level is significantly

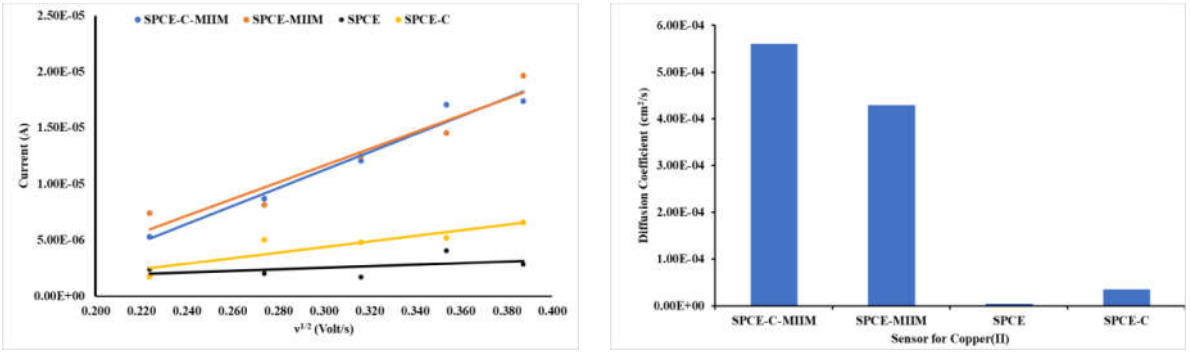

(a) (b)

FIGURE 7 The relationship of the square root of scan rate to peak current (a) and the diffusion coefficient of the sensor to Cu(II) (b) for 100 µM Cu(II) solution in 0.01 M KCl

higher than that of the second reduction (Figure 5). Hence, only the diffusion coefficient corresponding to the first reduction peak, which represents Cu(II) being reduced to Cu(I), is compared in the Cu(II) sensor. In terms of measurements, the application utilizes SWV technique and focuses on observing the first reduction peak. As illustrated in Figure 7b, it is evident that SPCE-C-MIIM's Cu(II) sensor exhibits the highest diffusion coefficient among other sensors tested. The addition of carbon paste enhances electron delivery conductivity due to the conductive nature of carbon (≈103 S/m) [67,68]. Consequently, the Cu(II) sensor can be labeled as SPCE-C-MIIP based on its diffusion coefficient.

Effect of pH

Understanding the impact of pH is crucial in investigating how the solubility of Cu(II) in water can be influenced. It has been observed that under acidic conditions, specifically at a pH range between 1 to 2, Cu(II) ions exhibit high solubility. At a slightly higher pH value of 3, the Cu(I) formation starts to occur and it still remains soluble in water. However, starting from a pH level of 6 onwards, the formation of Cu(II) takes place and its solubility decreases considerably (K_{sp} = 4.8 x 10^{-20}) [69,70].

In this particular study, observations were made within a range of pH values ranging from 2 to 5 using Britton Robinson buffer as an electrolyte support. The pH influence on the peak current of the SWV voltammogram can be observed in Figure 8. To compare the effects, both sensors (Cu(II) from SPCE-C-MIIM and Cu(II) from SPCE-MIIM) were studied alongside an SPCE as a control since their diffusion coefficients are similar. The linear regression equations presented in Table 1 were essential in this analysis, offering a quantitative framework to compare the performance of various Cu(II) sensors under different pH conditions.

The peak current (I_p) of the SWV voltammogram in SPCE is higher than in modified SPCE, but the data has a large deviation from 5 repetitions. At pH 2 the I_p of the modified SPCE is lower than the I_p at pH 3, and tends to decrease at pH 4 and 5. This may be caused by the charge of the Cu ion. At *p*H 2, the Cu ion in solution is dominated by Cu^{2+}, while at pH 3, it is dominated by $Cu(OH)^{+}$. It is estimated that the diffusion speed of $Cu(OH)^{+}$ is higher than Cu^{2+}, so that Ip is higher at pH 3. This does not happen at unmodified SPCE, because its surface is not selective . At pH 4 and 5 $Cu(OH)_2$ begins to form, so that the $Cu(OH)^{+}$ begins to decrease, as a result I_p decreases. The effect of pH in SPCE-MIIM and SPCE-C-MIIM, on I_p, has almost the same profile, but the deviation in SPCE-MIIM is higher.

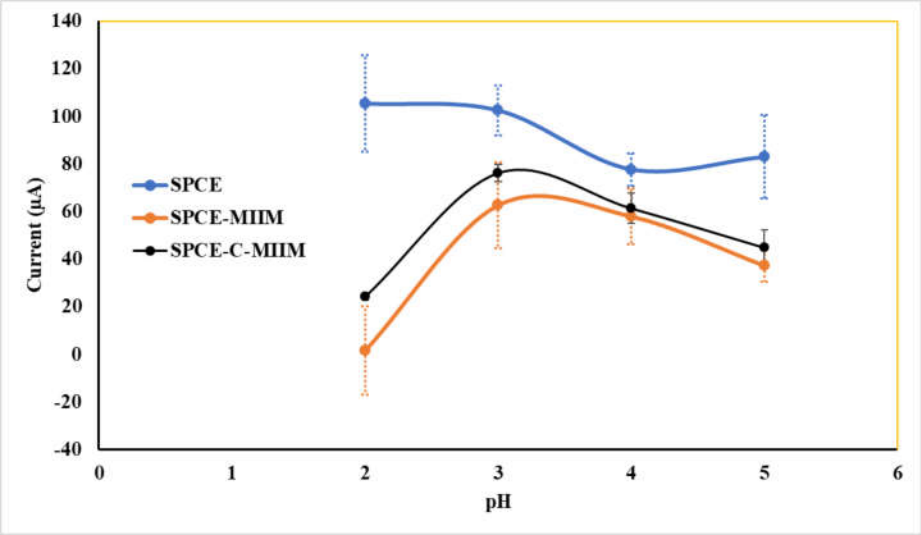

FIGURE 8 Relationship curve between *p*H and peak current of 100 µM Cu^{2+} solution in Britton Robinson buffer *p*H 2-5

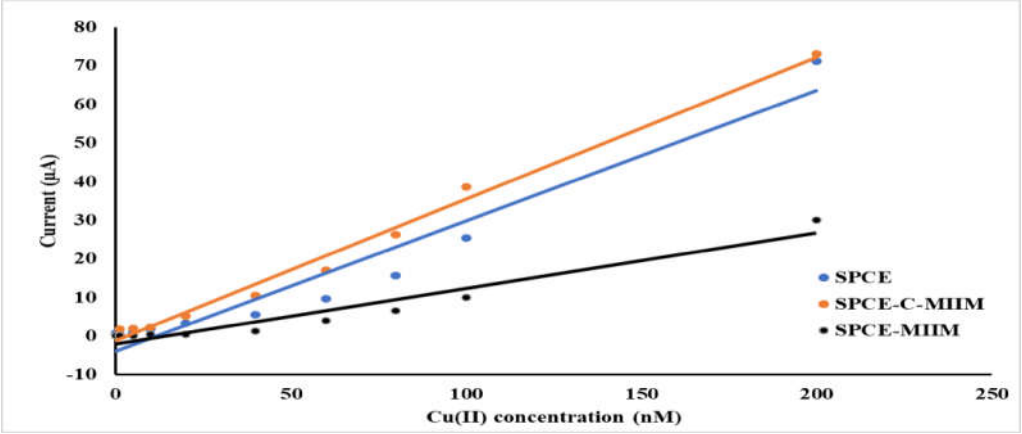

FIGURE 9 Relationship curve between Cu(II) concentration and SWV peak current for SPCE; SPCE-C-MIIM; and SPCE-MIIM

TABLE 1 Linear regression equations for various Cu(II) sensors

Sensor	Linear regression	R^2
SPCE	I_p = 0.3376 C	0.943
SPCE-C-MIIM	I_p = 0.3672 C	0.990
SPCE-MIIM	I_p = 0.144 C	0.936

The Cu(II) sensor performance

The detection of Cu(II) ions by square wave voltammetry method was performed on three different platforms: unmodified SPCE, SPCE modified by MIIP/Cu (referred to as SPCE-MIIP), and a paste made from carbon and MIIP/Cu (known as SPCE-C-MIIP). Figure 9 presents the SWV peak current obtained at various concentrations of Cu(II) at *p*H 3 in Britton Robinson buffer solution. The measurements were conducted using CV (cyclic voltammetry) and SWV (square wave voltammetry).

To evaluate the performance of the SPCE-C-MIIP sensor, a retest was conducted using various concentrations of Cu(II) ranging from 0 to 200 nM. by SWV method, the voltammogram shown in Figure 10a. From the voltammogram in Figure 10a, a standard curve was created, resulting a

regression equation $\mathbf{I_p = 0.49\ C}$ with a sensitivity of 0.49 µA/nM and a LoD is 3 nM. Sensor accuracy was determined by standard addition for three surface water samples. Each sample was added by 20 nM Cu(II), the voltammogram can be seen in Figure 10b. The sample's acidity was adjusted to *p*H 3 by Britton Robinson buffer in SWV analysis. The average accuracy of the standard addition results for the three water samples was (102.7±1.5)%.

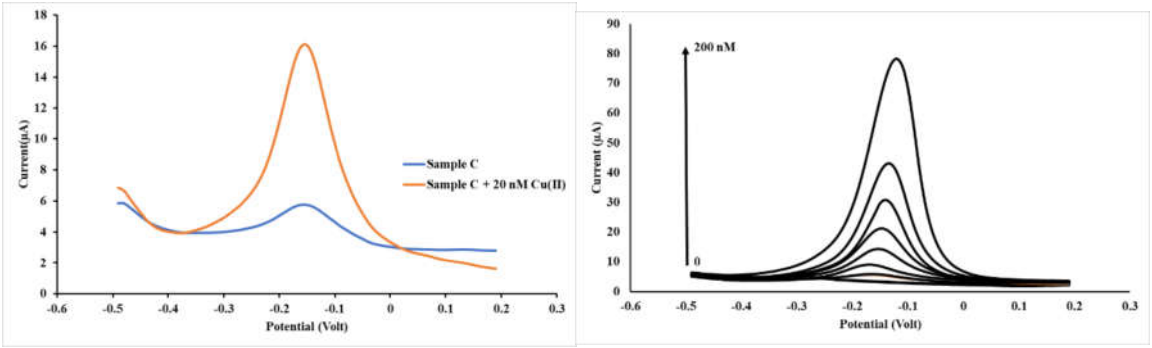

(a) (b)

FIGURE 10 Voltammograms of various Cu(II) concentrations at pH 3 (a), and voltammograms of samples and standard additions (b), resulted by the Cu(II) sensor of the SPCE-C-MIIP

Conclusion

To sum up, this study has successfully developed a novel electrochemical sensor that significantly enhances the detection of Cu(II) ions. The key innovation lies in the use of the Fe_3O_4@SiO_2-(Cu(II))-APTES composite (MIIM) and its integration with a screen-printed carbon electrode (SPCE). This combination, particularly when augmented with carbon paste, has led to remarkable improvements in sensitivity and accuracy over traditional SPCE sensors. The standout performer, the SPCE-C-MIIM sensor, showcases exceptional electrochemical properties, achieving high sensitivity, a remarkably low detection limit, and impressive accuracy under specific conditions. The significant advancements in detecting Cu(II) ions with these sensors, especially their potential application in analyzing surface water samples, mark a substantial step forward in environmental monitoring and public health protection. This breakthrough underscores the transformative impact of innovative material design and composite integration in enhancing the capabilities of electrochemical sensors.

Acknowledgments

The authors express gratitude to the Institute for Research and Community Service at Brawijaya University for providing financial support for this study through the PTNBH 2023 Collaboration Grant scheme. Grant of Program Penelitian Kolaborasi Indonesia-21 PTNBH for 2023 with contract number: 801.11/UN10.C10/TU/2023.

ORCID

Ani Mulyasuryani:
https://www.orcid.org/0000-0001-9984-0007
Matlal Fajri Alif:
https://www.orcid.org/0000-0003-2718-6880
Rahadian Zainul*:
https://www.orcid.org/0000-0002-3740-3597

References

[1]J. Baranwal, B. Barse, G. Gatto, G. Broncova, and A. Kumar, " Electrochemical sensors and their applications: A review, *Chemosensors*, **2022**, *10*, 363. [Crossref], [Google Scholar], [Publisher]

[2] O. Kanoun, T. Lazarević-Pašti, I. Pašti, S. Nasraoui, M. Talbi, A. Brahem, A. Adiraju, E. Sheremet, R.D. Rodriguez, M. Ben Ali, A. Al-Hamry, A review of nanocomposite-modified electrochemical sensors for water quality monitoring, *Sensors*, **2021**, *21*, 4131. [Crossref], [Google Scholar], [Publisher]

[3] R. Zainul, I.M. Isa, A.M. Yazid, S. Nur, N. Hashim, S.N. Mohd Sharif, M.I. Saidin, M.S. Ahmad, M.S. Suyanta, Y. Amir, Enhanced electrochemical sensor for electrocatalytic glucose analysis in orange juices and milk by the integration of the electron-withdrawing substituents on graphene/glassy carbon electrode, *Journal of Analytical Methods in Chemistry*, **2022**, *2022*. [Crossref], [Google Scholar], [Publisher]

[4] S. Brindred, M. Akhtarian Zand, Estimation of Sensor Bias Fault in Adaptive Control of Power System, *Eurasian Journal of Science and Technology*, **2021**, *1*, 20-27. [Crossref], [Publisher]

[5] A.A. Nurashikin, I.M. Isa, N. Hashim, M.S. Ahmad, R. Zainul, N.A.M.Y. Siti, S. Mukdasai, Synergistic Effect of Zinc/aluminium-layered Double Hydroxide-clopyralid Carbon Nanotubes Paste Electrode in the Electrochemical Response of Dopamine, Acetaminophen, and Bisphenol A, *International Journal of Electrochemical Science*, **2020**, *15*, 9088-9107. [Crossref], [Google Scholar], [Publisher]

[6] M., Sengar, Saxena, S., Satsangee, S., & Jain, R. Silver nanoparticles decorated functionalized multiwalled carbon nanotubes modified screen printed sensor for the voltammetric determination of butorphanol, *Journal of Applied Organometallic Chemistry*, **2021**, *1*, 95-108. [Crossref], [Google Scholar], [Publisher]

[7] S.N.A. Mohd Yazid, I. Md Isa, N.M. Ali, N. Hashim, M.I. Saidin, M.S. Ahmad, R. Zainul, Graphene/iridium (III) dimer complex composite modified glassy carbon electrode as selective electrochemical sensor for determination of hydroquinone in real-life water samples, *International Journal of Environmental Analytical Chemistry*, **2022**, *102*, 2607-2624. [Crossref], [Google Scholar], [Publisher]

[8] T. M. Adeniji and K. J. Stine, Nanostructure Modified Electrodes for Electrochemical Detection of Contaminants of Emerging Concern, *Coatings*, **2023**, *13*, 381. [Crossref], [Google Scholar], [Publisher]

[9] S. Kempahanumakkagari, A. Deep, K. H. Kim, S. Kumar Kailasa, and H. O. Yoon, Nanomaterial-based electrochemical sensors for arsenic-A review, *Biosensors and Bioelectronics*, **2017**, *95*, 106-116. [Crossref], [Google Scholar], [Publisher]

[10] S. Sharma, N. Singh, V. Tomar, and R. Chandra, A review on electrochemical detection of serotonin based on surface modified electrodes, *Biosensors and Bioelectronics*, **2018**, *107*, 76-93. [Crossref], [Google Scholar], [Publisher]

[11] N. S. M. Rais, I. M. Isa, N. Hashim, M. I. Saidin, S. N. A. M. Yazid, M. S. Ahmad, S. Mukdasai, Simultaneously determination of bisphenol A and uric acid by zinc/aluminum-layered double hydroxide-2-(2, 4-dichlorophenoxy) propionate paste electrode, *International Journal of Electrochemical Science*, **2019**, *14*, 7911-7924. [Crossref], [Google Scholar], [Publisher]

[12] R. Zainul, N. Hashim, S. N. A. M. Yazid, S. N. M. Sharif, M. S. Ahmad, M. I. Saidin, I.M. Isa, Magnesium layered hydroxide-3-(4-methoxyphenyl) propionate modified single-walled carbon nanotubes as sensor for simultaneous determination of Bisphenol A and Uric Acid, *International Journal of Electrochemical Science*, **2021**, *16*, 210941. [Crossref], [Google Scholar], [Publisher]

[13] N. Abd Azis, I. M. Isa, N. Hashim, M. S. Ahmad, S. N. A. M. Yazid, M. I. Saidin, S. Mukdasai, Voltammetric determination of bisphenol a in the presence of uric acid using a zn/al-ldh-qm modified MWCNT paste electrode, *International Journal of Electrochemical Science*, **2019**, *14*, 10607-10621. [Crossref], [Google Scholar], [Publisher]

[14] R. Zainul, N. Abd Azis, I. Md Isa, N. Hashim, M.S. Ahmad, M.I. Saidin, S. Mukdasai, Zinc/aluminium–quinclorac layered nanocomposite modified multi-walled carbon nanotube paste electrode for electrochemical determination of bisphenol A, *Sensors*, **2019**, *19*, 941. [Crossref], [Google Scholar], [Publisher]

[15] H. Hasanudin, W. R. Asri, I. S. Zulaikha, C. Ayu, A. Rachmat, F. Riyanti, R. Maryana, Hydrocracking of crude palm oil to a biofuel using zirconium nitride and zirconium phosphide-modified bentonite, *RSC Advances*, **2022**, *12*, 21916-21925. [Crossref], [Google Scholar], [Publisher]

[16] M. H. A. Tajudin, M. S. Ahmad, I. M. Isa, N. Hashim, A. Ul-Hamid, M. I. Saidin, S. M. Si, Sensitive determination of uric acid at layered zinc hydroxide-sodium dodecyl sulphate-propoxur nanocomposite, *Journal of Electrochemical Science and Engineering*, **2022**, *12*, 331-341. [Google Scholar], [Publisher]

[17] D. Rahmadiawan, H. Abral, M. K. Ilham, P. Puspitasari, R. A. Nabawi, S. C. Shi, R. Zainul, Enhanced UV blocking, tensile and thermal properties of bendable TEMPO-oxidized bacterial cellulose powder-based films immersed in PVA/Uncaria gambir/ZnO solution, *Journal of Materials Research and Technology*, **2023**, *26*, 5566-5575. [Crossref], [Google Scholar], [Publisher]

[18] A. D. Pournara, G. D. Tarlas, G. S. Papaefstathiou, and M. J. Manos, Chemically modified electrodes with MOFs for the determination of inorganic and organic analytes via voltammetric techniques: a critical review. *Inorganic Chemistry Frontiers*, **2019**, *6*, 3440-3455. [Crossref], [Google Scholar], [Publisher]

[19] J. Oguche, A. Ameh, T. Bello, N. Maina, Prospect of Deep Eutectic Solvents in Lactic Acid Production Process: A Review, *Journal of Chemical Reviews*, **2023**, *5*, 96-128. [Crossref], [Google Scholar], [Publisher]

[20] M. Ahmadlouydarab, S. Javadi, F. Adel Alijan Darab, Evaluation of Thermal Stability of TiO_2 Applied on the Surface of a Ceramic Tile to Eliminate Methylene Blue Using Silica-based Doping Materials, *Advanced Journal of Chemistry, Section A*, **2023**, *6*, 352-365. [Crossref], [Google Scholar], [Publisher]

[21] M. Manuel, A. Jennifer, A Review on Starch and Cellulose-Enhanced Superabsorbent Hydrogel, *Journal of Chemical Reviews*, **2023**, *5*, 183-203. [Crossref], [Google Scholar], [Publisher]

[22] I.H.I. Habib, M. Rizk, D. Mohamed, S. Mowaka, and R. T. El-Eryan, "Square wave voltammetric determination of rasagiline mesylate on hanging mercury drop electrode and its application in dosage form and biological fluids. *Int, J. Electrochem. Sci*, **2016**, *11*, 4802-4811. [Crossref], [Google Scholar], [Publisher]

[23] M. Majidian, J. B. Raoof, S. R. Hosseini, and R. Ojani, Determination of copper ion by square wave anodic stripping voltammetry at antimony trioxide-modified carbon nanotube paste electrode, *Journal of the Iranian Chemical Society*, **2017**, *14*, 1263-1270. [Crossref], [Google Scholar], [Publisher]

[24] S. Di Masi, A. Garcia Cruz, F. Canfarotta, T. Cowen, P. Marote, C. Malitesta, S.A. Piletsky, Synthesis and Application of Ion-Imprinted Nanoparticles in Electrochemical Sensors for Copper (II) Determination, *ChemNanoMat*, **2019**, *5*, 754-760. [Crossref], [Google Scholar], [Publisher]

[25] S.Theerthagiri, P. Rajkannu, P.S. Kumar, P. Peethambaram, C. Ayyavu, R. Rasu, D. Kannaiyan, Electrochemical sensing of copper (II) ion in water using bi-metal oxide framework modified glassy carbon electrode, *Food and Chemical Toxicology*, **2022**, *167*, 113313. [Crossref], [Google Scholar], [Publisher]

[26] S. Di Masi, A. Pennetta, A. Guerreiro, F. Canfarotta, G. E. De Benedetto, and C. Malitesta, Corrigendum to "Sensor based on electrosynthesised imprinted polymeric film for rapid and trace detection of copper (II) ions"[Sens. Actuators, B 307 127648](S0925400519318477)(10.1016/j. snb. 2019.127648). *SENSORS AND ACTUATORS. B, CHEMICAL*, **2020**, *311*, 1-1. [Crossref], [Google Scholar], [Publisher]

[27] M. Mazloum-Ardakani, M. K. Amini, M. Dehghan, E. Kordi, and M. A. Sheikh-Mohseni, Preparation of Cu (II) imprinted polymer electrode and its application for potentiometric and voltammetric determination of Cu (II), *Journal of the Iranian Chemical Society*, **2014**, *11*, 257-262. [Crossref], [Google Scholar], [Publisher]

[28] R. Zainul, B. Oktavia, I. Dewata, J. Efendi, April. Thermal and Surface Evaluation on The

Process of Forming a Cu2O/CuO Semiconductor Photocatalyst on a Thin Copper Plate. In *IOP Conference Series: Materials Science and Engineering*, **2018**, *335*, 12039 [Crossref], [Google Scholar], [Publisher]

[29] A. Bhagi-Damodaran, J.H. Reed, Q. Zhu, Y. Shi, P. Hosseinzadeh, B.A. Sandoval, K.A. Harnden, S. Wang, M.R. Sponholtz, E.N. Mirts, S. Dwaraknath, Heme redox potentials hold the key to reactivity differences between nitric oxide reductase and heme-copper oxidase, *Proceedings of the National Academy of Sciences*, **2018**, *115*, 6195-6200. [Crossref], [Google Scholar], [Publisher]

[30] N. Rasouli, H. Salavati, M. Movahedi, A. Rezaei, An Insight on Kinetic Adsorption of Congo Red Dye from Aqueous Solution using Magnetic Chitosan Based Composites as Adsorbent, *Chemical Methodologies*, **2017**, *1*, 74-86. [Crossref], [Google Scholar], [Publisher]

[31] O. Daliri Shamsabadi, Investigation of Antimicrobial Effect and Mechanical Properties of Modified Starch Films, Cellulose Nanofibers, and Citrus Essential Oils by Disk Diffusion Method, *Asian Journal of Green Chemistry*, **2024**, *8*, 1-14. [Crossref], [Publisher]

[32] L. A. Escudero, S. Cerutti, R. A. Olsina, J. A. Salonia, and J. A. Gasquez, Factorial design optimization of experimental variables in the on-line separation/preconcentration of copper in water samples using solid phase extraction and ICP-OES determination, *Journal of Hazardous Materials*, **2010**, *183*, 218-223. [Crossref], [Google Scholar], [Publisher]

[33] Y. L. Yu and J. H. Wang, Recent advances in flow-based sample pretreatment for the determination of metal species by atomic spectrometry, *Chinese Science Bulletin*, **2013**, *58*, 1992-2002. [Crossref], [Google Scholar], [Publisher]

[34] C. Branger, W. Meouche, A. Margaillan, Recent advances on ion-imprinted polymers, *Reactive and Functional Polymers*, **2013**, *73*, 859-875. [Crossref], [Google Scholar], [Publisher]

[35] P. Wei, Z. Zhu, R. Song, Z. Li, C. Chen, An ion-imprinted sensor based on chitosan-graphene oxide composite polymer modified glassy carbon electrode for environmental sensing application, *Electrochimica Acta*, *317*, pp.93-101 [Crossref], [Google Scholar], [Publisher]

[36] A. Shouli, S. Menati, S. Sayyahi, Copper (II) chelate-bonded magnetite nanoparticles: A new magnetically retrievable catalyst for the synthesis of propargylamines, *Comptes Rendus Chimie*, **2017**, *20*, 765-772. [Crossref], [Google Scholar], [Publisher]

[37] X. Luo, S. Luo, Y. Zhan, H. Shu, Y. Huang, and X. Tu, Novel Cu (II) magnetic ion imprinted materials prepared by surface imprinted technique combined with a sol–gel process, *Journal of Hazardous Materials*, **2011**, *192*, 949-955. [Crossref], [Google Scholar], [Publisher]

[38] M. J. Kuras and E. Więckowska, Synthesis and characterization of a new copper (II) ion-imprinted polymer, *Polymer Bulletin*, **2015**, *72*, 3227-3240. [Crossref], [Google Scholar], [Publisher]

[39] X. Zhou, B. Wang, and R. Wang, Insights into ion-imprinted materials for the recovery of metal ions: Preparation, evaluation and application, *Separation and Purification Technology*, **2022**, *298*, 121469. [Crossref], [Google Scholar], [Publisher]

[40] A. Sala, H. Brisset, A. Margaillan, J.U. Mullot, C. Branger, Electrochemical sensors modified with ion-imprinted polymers for metal ion detection. TrAC Trends in Analytical Chemistry, **2022**, *148*, 116536 [Crossref], [Google Scholar], [Publisher]

[41] A. Abdul Halim, S.S. Sulaiman, A.N. Nordin, H. Bajunaid Hariz, Systematic review study on application of Ion Imprinted Polymer (IIP) in heavy metals detection, *International Journal of Environmental Analytical Chemistry*, **2022**, 1-25. [Crossref], [Google Scholar], [Publisher]

[42] M. Hong, X. Wang, W. You, Z. Zhuang, and Y. Yu, Adsorbents based on crown ether functionalized composite mesoporous silica for selective extraction of trace silver, *Chemical Engineering Journal*, **2017**, *313*, 1278-1287. [Crossref], [Google Scholar], [Publisher]

[43] Q. Li, H. Su, and T. Tan, Synthesis of ion-imprinted chitosan-TiO2 adsorbent and its

multi-functional performances, *Biochemical Engineering Journal*, **2008**, *38*, 212-218. [Crossref], [Google Scholar], [Publisher]

[44] H. Ebrahimzadeh, A. A. Asgharinezhad, E. Moazzen, M. M. Amini, O. Sadeghi, A magnetic ion-imprinted polymer for lead (II) determination: A study on the adsorption of lead (II) by beverages, *Journal of Food Composition and Analysis*, **2015**, *41*, 74-80. [Crossref], [Google Scholar], [Publisher]

[45] A. Kiani and M. Ghorbani, Synthesis of core–shell magnetic ion-imprinted polymer nanospheres for selective solid-phase extraction of Pb2+ from biological, food, and wastewater samples, *Journal of Dispersion Science and Technology*, **2017**, *38*, 1041-1048. [Crossref], [Google Scholar], [Publisher]

[46] Y. Cui, L. Ding, and J. Ding, Recent advances of magnetic molecularly imprinted materials: From materials design to complex sample pretreatment, *TrAC Trends in Analytical Chemistry*, **2022**, *147*, 116514. [Crossref], [Google Scholar], [Publisher]

[47] H. Zhao, Q. Liang, Y. Yang, W. Liu, and X. Liu, Magnetic graphene oxide surface lithium ion-imprinted material towards lithium extraction from salt lake, *Separation and Purification Technology*, **2021**, *265*, 118513. [Crossref], [Google Scholar], [Publisher]

[48] Z. Zhao, H. Jiang, L. Wu, N. Yu, Z. Luo, W. Geng, Preparation of Magnetic Surface Ion-Imprinted Polymer Based on Functionalized Fe3O4 for Fast and Selective Adsorption of Cobalt Ions from Water, *Water*, **2022**, *14*, 26. [Crossref], [Google Scholar], [Publisher]

[49] S. Liu, B. Yu, S. Wang, Y. Shen, and H. Cong, Preparation, surface functionalization and application of Fe3O4 magnetic nanoparticles. *Advances in colloid and Interface Science*, **2020**, *281*, 102165. [Crossref], [Google Scholar], [Publisher]

[50] N. Kurnaz Yetim, F. Kurşun Baysak, M. M. Koç, D. Nartop, Characterization of magnetic Fe 3 O 4@ SiO 2 nanoparticles with fluorescent properties for potential multipurpose imaging and theranostic applications. *Journal of Materials Science, Materials in Electronics*, **2020**, *31*, 18278-18288. [Crossref], [Google Scholar], [Publisher]

[51] Z. Wang, C. Zhou, S. Wu, and C. Sun, Ion-imprinted polymer modified with carbon quantum dots as a highly sensitive copper (II) Ion Probe, *Polymers*, **2021**, *13*, 1376 [Crossref], [Google Scholar], [Publisher]

[52] Z. Zhao, H. Jiang, L. Wu, N. Yu, Z. Luo, W. Geng, Preparation of Magnetic Surface Ion-Imprinted Polymer Based on Functionalized Fe3O4 for Fast and Selective Adsorption of Cobalt Ions from Water, *Water*, **2022**, *14*, 261. [Crossref], [Google Scholar], [Publisher]

[53] Y. Li, X. Li, J. Chu, C. Dong, J. Qi, Y. Yuan, Synthesis of core-shell magnetic molecular imprinted polymer by the surface RAFT polymerization for the fast and selective removal of endocrine disrupting chemicals from aqueous solutions, *Environmental Pollution*, **2010**, *158*, 2317-2323 [Crossref], [Google Scholar], [Publisher]

[54] A. Mulyasuryani and D. E. Dwi Prasetya, June. Development of Chemical sensor for detection of monosodium glutamate by polyvinyl alcohol-Fe3O4 membrane on screen printed carbon electrode, In *IOP Conference Series: Materials Science and Engineering* , **2019**, *546*, 32022 [Crossref], [Google Scholar], [Publisher]

[55] A. Mulyasuryani and A. M. Mustaghfiroh, Development of potentiometric phenol sensors by nata de coco membrane on screen-printed carbon electrode, *Journal of analytical methods in chemistry*, **2019**, *2019* [Crossref], [Google Scholar], [Publisher]

[56] S. Ariavand, M. Ebrahimi, E. Foladi, Design and Construction of a Novel and an Efficient Potentiometric Sensor for Determination of Sodium Ion in Urban Water Samples, *Chemical Methodologies*, **2022**, *6*, 886-904. [Crossref], [Google Scholar], [Publisher]

[57] Vardini, M. T., Abbasi, N., Kaviani, A., Ahmadi, M., & Karimi, E., Graphite electrode potentiometric sensor modified by surface imprinted silica gel to measure valproic acid, *Chemical Methodologies*, **2022**, *6*, 398-408. [Crossref], [Google Scholar], [Publisher]

[58] E. E. Krisnaningrum, A. Mulyasuryani, H. Sulistyarti, Modification of Electrode using Arrowroot Starch Membrane for Uric Acid

Determination, *Molekul*, **2021**, *16*, 186-193. [Crossref], [Google Scholar], [Publisher]
[59] A. Mulyasuryani, Y. P. Prananto, Q. Fardiyah, H. Widwiastuti, D. Darjito, Application of Chitosan-Based Molecularly Imprinted Polymer in Development of Electrochemical Sensor for p-Aminophenol Determination, *Polymers*, **2023**, *15*, 1818 [Crossref], [Google Scholar], [Publisher]
[60] K. Yang, H. Peng, Y. Wen, N. Li, Re-examination of characteristic FTIR spectrum of secondary layer in bilayer oleic acid-coated Fe3O4 nanoparticles, *Applied surface science*, **2010**, *256*, 3093-3097 [Crossref], [Google Scholar], [Publisher]
[61] S. Arief, M. Muldarisnur, S.R. Usna, Enhancement in photoluminescence performance of carbon-based Fe3O4@ ZnO–C nanocomposites. Vacuum, **2023**, *211*, 111935. [Crossref], [Google Scholar], [Publisher]
[62] A. B. D. Nandiyanto, R. Oktiani, R. Ragadhita, How to read and interpret FTIR spectroscope of organic material, *Indonesian Journal of Science and Technology*, **2019**, *4*, 97-118. [Crossref], [Google Scholar], [Publisher]
[63] R. Khatun, M.S.A. Mamun, S. Islam, N. Khatun, M. Hakim, M.S. Hossain, P.K. Dhar, H.R. Barai, Phytochemical-assisted Synthesis of Fe3O4 Nanoparticles and Evaluation of Their Catalytic Activity, *Micromachines*, **2022**, *13*, 2077. [Crossref], [Google Scholar], [Publisher]
[64] H. Yamada, K. Yoshii, M. Asahi, M. Chiku, and Y. Kitazumi, Cyclic Voltammetry Part 2: Surface Adsorption, Electric Double Layer, and Diffusion Layer, *Electrochemistry*, **2022**, *90*, 102006-102006. [Crossref], [Google Scholar], [Publisher]
[65] F. Rahmawati, K.R. Heliani, A.T. Wijayanta, R. Zainul, K. Wijaya, Miyazaki, T. and Miyawaki, J., 2023. Alkaline leaching-carbon from sugarcane solid waste for screen-printed carbon electrode, *Chemical Papers*, **2023**, *77*, 3399-3411. [Google Scholar], [Publisher]
[66] R.M. Bhattarai, K. Chhetri, S. Natarajan, S. Saud, S.J. Kim, Y.S. Mok, Activated carbon derived from cherry flower biowaste with a self-doped heteroatom and large specific surface area for supercapacitor and sodium-ion battery applications, *Chemosphere*, **2022**, *303*, 135290. [Crossref], [Google Scholar], [Publisher]
[67] B. Marinho, M. Ghislandi, E. Tkalya, C. E. Koning, and G. de With, Electrical conductivity of compacts of graphene, multi-wall carbon
[68] nanotubes, carbon black, and graphite powder, *Powder technology*, **2012**, *221*, 351-358. [Crossref], [Google Scholar], [Publisher]
[69] K. Wijaya, R.A. Pratika, A. Nadia, F. Rahmawati, R. Zainul, W.C. Oh, W.D. Saputri, Recent Trends and Application of Nanomaterial Based on Carbon Paste Electrodes: A Short Review, **2023**[Crossref], [Google Scholar], [Publisher]
[70] J. D. Cuppett, S. E. Duncan, and A. M. Dietrich, Evaluation of copper speciation and water quality factors that affect aqueous copper tasting response, *Chemical senses*, **2006**, *31*, 689-697. [Crossref], [Google Scholar], [Publisher]
[71] M.C. Sheikh, M.M. Hasan, M.N. Hasan, M.S. Salman, K.T. Kubra, M.E. Awual, R.M. Waliullah, A.I. Rasee, A.I. Rehan, M.S. Hossain, H.M. Marwani, Toxic cadmium (II) monitoring and removal from aqueous solution using ligand-based facial composite adsorbent. *Journal of Molecular Liquids*, **2023**, *389*, 122854. [Crossref], [Google Scholar], [Publisher]

How to cite this article: Ani Mulyasuryani, Matlal Fajri Alif , Rahadian Zainul*, Novel electrochemical sensor of Cu(II) prepared by carbon paste-magnetic ion imprinted materials on screen printed carbon electrode. *Journal of Medicinal and Pharmaceutical Chemistry Research* , 2024, 6(5), 502-518.
Link: http://jmpcr.samipubco.com/article_186624.html

Copyright © 2024 by SPC (Sami Publishing Company) + is an open access article distributed under the Creative Commons Attribution License(CC BY) license (https://creativecommons.org/licenses/by/4.0/), which permits unrestricted use, distribution, and reproduction in any medium, provided the original work is properly cited.